Dynamics and fluctuations during MBE on vicinal surfaces. I. Formalism and results of linear theory

O. Pierre-Louis* and C. Misbah
Laboratoire de Spectrométrie Physique, Université Joseph Fourier, CNRS, Grenoble I, Boîte Postale 87, Saint-Martin d'Hères, 38402 Cedex, France
(Received 28 July 1997; revised manuscript received 30 December 1997)

We develop a full nonlinear theory including fluctuations for the study of dynamics of vicinal surfaces during molecular beam epitaxy. We consider the situation where the surface grows through step flow. The model is based on the Burton-Cabrera-Frank one, in which kinetic attachments, elastic interactions, and statistical fluctuations, through Langevin forces, are incorporated. Green's functions techniques are used. The step dynamics are governed in the general case by nonlinear and nonlocal coupled equations. At equilibrium we recover known results and some of them are revisited. For example, we find that the step meander behaves at equilibrium as $w \sim l^{\alpha}[\ln(L)]^{1/2}$ (l is the mean interstep distance and L the lateral step extent). The quantity $\alpha = 1/2$ or 1 depending on whether the elastic interaction is $\ln(l)$ or $1/l^2$. During step flow growth the steps repel each other via the diffusion field. This repulsion prevails over the elastic one. It leads to an exponent 1/4; $w \sim l^{1/4}$. Because the diffusive repulsion is much bigger than the elastic one, nonequilibrium conditions should first result in a drastic reduction of the vicinal surface fluctuation (steps wandering and terrace width fluctuations). However, on further increase of the incoming flux F, the steps become morphologically unstable. This instability is driven by adatom diffusion. It is of deterministic origin and must be distinguished from purely statistical fluctuations. At the instability threshold and in the linear regime, the roughness behaves as $w \sim \epsilon^{-1/2} L^{1/2}$ (ϵ is the distance from the instability threshold) for an isolated step and $w \sim \epsilon^{-1/4}[\ln(L)]^{1/2}$ for a train of steps. The exponent 1/4 is a direct consequence of step-step interaction. At the instability point nonlinear terms become relevant. The nonlinear regime is discussed in detail in the following paper. [S0163-1829(98)06027-5]

I. INTRODUCTION

Many semiconductors are produced by molecular beam epitaxy (MBE). Understanding of how and by which mechanisms production of solids is often hampered by deterministic and stochastic roughness is of a paramount importance on the technological level. Indeed, one of the main objectives of MBE is to produce abrupt surfaces on the atomic scales for several application. This is, however, altered in several instances by the appearance of undesirable roughness, which may be of either stochastic or deterministic nature. There are situations, however, where such roughness may become very advantageous. This is the case of the fabrication of quantum dots, which is a topic of much current interest. At the same time this problem raises challenging and subtle questions of fundamental nonequilibrium statistical physics.

The advent of microscopic techniques such as scanning tunneling microscopy (STM) and reflection electron microscopy has induced a surge of interest in the study of both structural and dynamical properties of surfaces. Growth of solids with atomically controlled morphologies can proceed either on a high symmetry singular surface or on a vicinal (stepped) surface. The latter situation offers, in principle, the advantage of producing layer by layer growth through step flow. It can also be used to produce low-dimensional architectures such as quantum wires due to the availability of nucleation centers along the steps. There is now ample evidence that during many technologically important processes (such as growth and reaction) steps play an active role. For this reason considerable attention, both experimental and theoretical, is being devoted to this topic. This paper will focus on the dynamics of vicinal surfaces during MBE. More precisely, our study concerns surface growth through step flow. Several behaviors will emerge. For example, nonequilibrium conditions lead (if the incoming flux is not too large) to a drastic reduction of the surface fluctuations. That is to say, the steps wandering and terrace width fluctuations are significantly reduced as soon as the system is driven away from equilibrium. If the incoming flux is large enough [e.g., a few monolayers per second for Si(111) at $T \sim 600$ °C] different phenomena appear: These are morphological instabilities due to nonequilibrium conditions that cause the step profile to become unstable against protuberance. This may either not affect too much step-flow growth or, on the contrary, result ultimately in a largely rough surface through secondary instabilities, depending on the regions in parameter space.

The most noticeable feature of a step is its meander. Meandering is manifest from STM visualization[1] for example. The relatively important step wandering is due to the one-dimensional character of the step; an isolated step is expected to be rough at all temperatures at large scales. For example, an isolated step wanders at equilibrium on average a distance $\sqrt{L}$ from its flat configuration. Fluctuations in the step profile $z = \zeta(x)$ are governed by the Boltzmann distribution

$$P\{\zeta\} \sim \exp\left(\frac{-(\gamma/2)\int_0^L [\partial_x \zeta]^2 dx}{k_B T} \right),$$

where γ is the free energy per unit length of step and T the temperature (we consider the case where γ is isotropic). This distribution yields trivially the static fluctuation spectrum $\langle \zeta_k \zeta_{-k} \rangle_s = k_B T/\gamma k^2$, where $k = 2n\pi/L$, and the step width $w_s \equiv (\langle \zeta^2 \rangle_{\rm eq})^{1/2}$ via the relation

$$w_s^2 = \frac{k_B T L}{12\gamma}. \tag{1}$$

This result is akin to the Brownian motion of a particle[2] whose trajectory suffers excursions that increase as $\sqrt{t}$ in the course of time or a polymer whose meander ''diverges'' with the number of monomers as $\sqrt{N}$.

In a train, like on a vicinal surface, the steps interact with each other. At equilibrium, most important is the elastic interaction, which behaves either as $1/l^2$ (l is the interstep distance)[4] or $\ln(l)$. The former case concerns homoepitaxy with the same atomic environment on each terrace. The second case should show up either (i) in the case where a film is on top of a vicinal substrate or (ii) if two adjacent terraces have different structures and/or properties (see below). A typical example is Si(001), which is known to show a reconstruction (1×2)-(2×1); from one terrace to the next the dimer rows are perpendicular to each other. Elastic repulsion may limit the wandering of a step. A step forward was conducted by Bartelt *et al.*,[5] who provided an expression for the meander w_s as a function of relevant parameters (written here for an elastic repulsion $\sim 1/l^2$)

$$w_s = \left[\frac{(k_B T)^2}{8\gamma \hat{\mathcal{A}}} \right]^{1/4} l, \tag{2}$$

where $\hat{\mathcal{A}}$ is the strength of the elastic interaction. This expression was derived for a wandering step between two rigid ones. A typical example would be the case of Si(001). In general, however, steps execute collective motions and all relative fluctuations are allowed. It will emerge in this paper that if all motions are allowed, the meander takes the form

$$w_s' \simeq \frac{l}{\sqrt{2\pi}} \left[\frac{(k_B T)^2}{\gamma \hat{\mathcal{A}}} \right]^{1/4} [\ln(L\tilde{a}/l^2)]^{1/2}, \tag{3}$$

where $\tilde{a}$ is an atomic distance. This result shows that allowing for all motions converts the $\sqrt{L}$ behavior typical for an isolated step into a logarithmic divergence, which is characteristic of a two-dimensional problem. On the other hand, for a given L, there are logarithmic corrections as far as the dependence on the tilt angle (or the interstep distance) is concerned.

During growth by MBE, the mechanisms that control the evolution of the growth morphology include in addition deposition, diffusion of adatoms, desorption, and the sticking kinetics at the steps. This process of evolution of surfaces by the addition of particles is a prototype of problems in open nonequilibrium systems where the traditional approach of equilibrium statistical mechanics is difficult to apply. The first aim of this paper is to present the general formulation of step dynamics including the relevant ingredients, together with an appropriate Langevin formalism for the different sources of noise (shot noise, diffusion noise, and attachment/detachment noise at the steps), on which we have given recently a brief account.[6] The general resulting dynamical equations are coupled nonlinear and nonlocal stochastic equations for the instantaneous step positions. We shall exploit them in the linear and weakly nonlinear regimes.

In the linear regime (where the deposition flux is small enough), diffusion (which is a passive quantity at equilibrium) becomes active: It leads to repulsion between steps. We shall refer to it as *diffusive repulsion*. This repulsion can be understood as follows. First, usually adatoms that come from the lower terrace are more easily incorporated in the step than those coming from the upper one. This is due to the Ehrlich-Schwœbel (ES) effect.[7] In the following reasoning presented in this introduction, we assume that only adatoms belonging to the lower terrace contribute to step motion (the one-sided model). The mass current at the step is (when the diffusion length defined as $x_s = \sqrt{D\tau}$, where D is the adatom diffusion constant and τ atomic desorption rate, is bigger than the interstep distance l) proportional to l, the terrace width ahead of the step. If this terrace width becomes larger (due to some fluctuation) than that of the two adjacent ones, this implies that it will immediately shrink since the step velocity of the upper step (the ascending one) will be larger. Conversely, if the width becomes smaller, the ascending step decelerates, leading thereby to a terrace width increase. The response of the step to terrace width fluctuations is mediated by the diffusion field. This phenomenon can be viewed as the result of a diffusive repulsion. We shall see that for typical deposition fluxes, the diffusive repulsion prevails over the elastic one. As a consequence, the step meander is no longer controlled by the elastic repulsion (except for large tilt angles), but rather by diffusion. We shall show that the dynamical meander behaves typically as (for a small Schwœbel effect and where adatoms are supposed to instantaneously stick to the ascending step)

$$w_D = \left(\frac{\Omega D c_{eq}^0 k_B T}{2\gamma d^2 F} \right)^{1/4} l^{1/4}, \tag{4}$$

where Ω is the atomic area, c_{eq}^0 the equilibrium adatom concentration, F the deposition rate, D the adatom diffusion constant, and $d = D/\nu$ the Schwœbel length (ν is the sticking kinetic coefficient for the descending atoms). The presence of D/F together with d above signals the nonequilibrium nature of the mechanism by which the meander is fixed. Since, as we stated, the diffusive repulsion is larger than the elastic one, we expect the nonequilibrium meander to be reduced. That is to say, nonequilibrium effects (for not too large fluxes) should first lead to a smoothening of the steps. This should constitute the first noticeable qualitative feature to be observed in experiments. In an analogy with equilibrium theory, we shall see that the repulsive diffusion in this regime should behave like $l\ \ln(l)$.

On further increasing the incoming flux, diffusion causes a morphological instability of the steps, as shown by Bales and Zangwill.[8] This is the one-dimensional analog of the Mullins-Sekerka[9] instability. We shall give here a very transparent condition for the instability onset. The critical flux is fixed by a ratio between a length associated with the (stabilizing) line tension ($\Gamma = \Omega^2 c_{eq}^0 \gamma/k_B T$) over the smallest destabilizing length in the problem: the diffusion length x_s, the

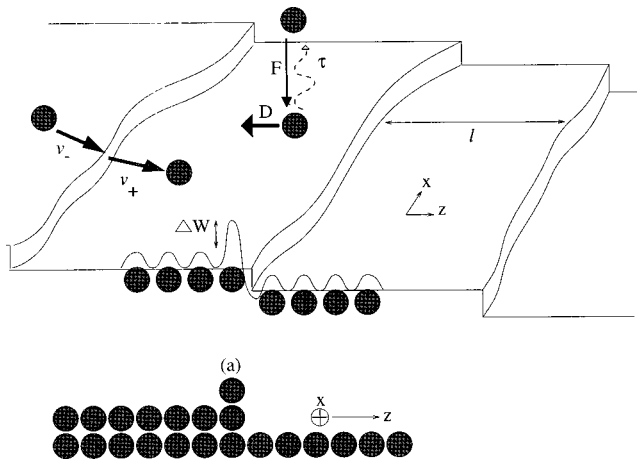

FIG. 1. F is the flux of atoms landing on the terraces. The adatoms diffuse on the terraces with the diffusion constant D. Their characteristic wandering time before evaporation is τ. Attachment-detachment processes are characterized by kinetic coefficients $\nu_{\pm}$ on both sides of the steps. To stick to a step, the adatom coming from the upper terrace has to go through a position (a), which is energetically unfavorable because it has fewer neighbors. The adatoms therefore have to surmount an additional energy barrier ΔW. This is called the Erlich-Schwœbel effect and leads to a difference between the kinetic coefficients $\nu_{+} > \nu_{-}$.

ES length d, or the interstep length l. In the linear regime and at the instability threshold, the meander is expected to diverge, which is a natural consequence of an instability.[10] If ϵ denotes the departure from the critical flux, the meander for an isolated step[10] diverges like $w_D \sim \epsilon^{-1/2}$. We shall show that in a train of steps, we have $w_D \sim \epsilon^{-1/4}$ instead.

As the threshold is approached fluctuations become arbitrarily large so that disregarding nonlinearities is illegitimate. The nonlinear treatment is presented in detail in the following paper.

The scheme of this paper is as follows. In Sec. II we write down and comment on the model equations. We shall then make use of a Green's function formalism to establish an integral dynamical equation describing steps dynamics. In Sec. III we deal with the linear problem and derive a nonlocal linear Langevin equation. In Sec. IV we recall known results at equilibrium and present different features. Section V is devoted to the out-of-equilibrium regime. The main results are summed up in Sec. VI. Many lengthy expressions together with several technical manipulations are relegated to the Appendixes.

II. MODEL

A. Model equations

Figure 1 represents a typical vicinal surface. In the Burton-Cabrera-Frank[11] model, incoming adatoms diffuse on the terrace with a diffusion constant D, may evaporate with a frequency $1/\tau$, and stick instantaneously to the steps. The growth operates in a regime known as *step flow*. Step flow occurs at not too low temperature and for not too large terrace width; otherwise two-dimensional island formation takes place. We will return to this point in the discussion.

In general, the adatoms stick more easily when they come from the lower side than from the upper one (this is the Ehrlich-Schwœbel[7] effect). This effect leads to several important features and will be included here. Moreover, steps interact with each other (even at equilibrium) through the elastic field. This may lead to meander restrictions. This effect can show up in particular in a regime where steps form bunches (step bunching is not discussed here) or when the misorientation angle is large. On the other hand elastic interactions should often play a decisive role in the choice of surface morphologies and their effects must be estimated. Finally, on the one hand, adatoms have ample time to diffuse to highly coordinated lattice sites between two deposition events and a smooth morphology is expected. However, both shot noise and the (conserved) diffusive noise will always reinstitute themselves to roughen the steps on some scales. Moreover, adatoms are attached more easily to existing protuberances, thereby leading to morphological instabilities. These instabilities may ultimately result in a completely rough surface. Crystal morphologies are the result of a subtle interplay between thermodynamic (e.g., elastic effects) and kinetic (e.g., deposition and diffusion) effects of both stochastic and deterministic origins.

Let us now introduce the model equations. Let c denote the areal (number of adatoms per unit surface) adatom concentration on the terraces. It obeys, in the general case, the stochastic equation

$$\frac{\partial c}{\partial t} = D\nabla^2 c - \frac{c}{\tau} + F + f - \boldsymbol{\nabla}\cdot\mathbf{q}. \tag{5}$$

While the quasisteady approximation (setting the left-hand side equal to zero) is often legitimate (see later), we shall keep for the moment the full dynamical equation. Here τ^{-1} is the desorption rate, D is the diffusion constant of the adatoms, and F is the adatom incoming flux. The other terms are f, a shot noise related to the adsorption/desorption process, and $\mathbf{q}$, a conserved noise associated with fluctuations of the diffusion current. We shall specify below the amplitudes of these stochastic quantities. It must be mentioned at this stage that both the nonconserved and the conserved noise are crucial for the large scale dynamics, contrary to what is stated in Ref. 12. Indeed, while the diffusion along the steps is irrelevant at large scales (as one can intuitively expect), diffusion in the orthogonal direction is relevant at all scales. The orthogonal part plays for the steps a very similar role to that due to a deposition flux for growth on a surface.

On both sides of the steps, the incoming adatom flux is linearly related to the departure from equilibrium. In a picture in the manner of Onsager,

$$\mp\mathbf{n}\cdot(-D\boldsymbol{\nabla}c+\mathbf{q})_{\pm} = \nu_{\pm}(c - c_{eq} + \eta_{\pm}), \tag{6}$$

where $\eta_{\pm}$ are attachment-detachment Langevin forces, $\mathbf{n}$ is the unit normal vector at the step pointing from the upper terrace into the lower one, and $\nu_{\pm}$ are phenomenological kinetic coefficients having the dimension of a velocity.

In expression (6) c_{eq} refers to the equilibrium concentration at a step modified by interactions with the neighboring steps as well as by curvature effects. Let c_{eq}^0 denote the equilibrium concentration of an isolated straight step. At equilibrium, the chemical potentials of the adatoms on the terraces μ_g and atoms in the crystal μ_s are equal:

$$\mu_s(p_s)=\mu_g(p_g,c_{eq}), \tag{7}$$

where p_s and p_g are the pressures at the step on the solid side and in the gas atmosphere, respectively. For small departures from equilibrium one expects that a linear expansion of the chemical potential[15] difference is legitimate. For small deviations from the equilibrium reference point $c=c_{eq}^0$ and $p=p_g$, a linear expansion of Eq. (7) leads to

$$(p_s-p_g)\left(\frac{\partial\mu_s}{\partial p}\right)_{p_g,c_{eq}^0}=(c_{eq}-c_{eq}^0)\left(\frac{\partial\mu_g}{\partial c}\right)_{p_g,c_{eq}^0}. \tag{8}$$

The derivatives can be expressed explicitly. Indeed, $\partial\mu_s/\partial p=\Omega$ is the atomic area (this is an exact thermodynamic quantity). In the ideal gas approximation $\partial\mu_g/\partial c=k_BT/c_{eq}^0$. The total mechanical equilibrium involves the hydrostatic pressure together with other forces (e.g., the elastic ones). If $\mathcal{E}$ refers to the total energy modified by the line stiffness and elastic effects, then mechanical equilibrium implies

$$p_s-p_g=\frac{\delta\mathcal{E}}{\delta\zeta_m}, \tag{9}$$

where $\mathcal{E}$ takes the form (we assume here that the step-step interaction is inversely proportional to the square of the distance)

$$\mathcal{E}=\sum_{m=-\infty}^{+\infty}\int_0^L dx\left\{\gamma\left[1+\left(\frac{\partial\zeta_m}{\partial x}\right)^2\right]^{1/2}+\frac{\hat{\mathcal{A}}}{6}\frac{1}{(l-\zeta_m+\zeta_{m+1})^2}\right\}, \tag{10}$$

where m labels a step, l is the mean interstep distance, and γ is the step line tension. We disregard here anisotropy effects, which can easily be incorporated in the model. For the sake of simplicity, we use a first-neighbor interaction approximation. A generalization to further neighbors is readily made. The order of magnitude of these energies is simply extracted from a dimensional analysis. γ and $\hat{\mathcal{A}}$ can be related to a macroscopic quantity, namely, the Young modulus $E\sim10^{10}$ Pa and an atomic length $a\sim3\times10^{-10}$ m (for silicon). From a dimensional analysis, we have $\gamma\sim Ea^2\sim10^{-9}$ J m^{-1} and $\hat{\mathcal{A}}\sim Ea^4\sim10^{-28}$ J m. Note that since $a<l$, $\hat{\mathcal{A}}/l^2<\gamma$ because $\hat{\mathcal{A}}/\gamma l^2\sim(a/l)^2<1$. With the help of Eq. (10), Eq. (9) can be rewritten as

$$p_s-p_g=\gamma\kappa_m+\frac{\hat{\mathcal{A}}}{3}\left(\frac{1}{(l+\zeta_{m+1}-\zeta_m)^3}-\frac{1}{(l+\zeta_m-\zeta_{m-1})^3}\right), \tag{11}$$

where κ_m is the step curvature counted to be positive for a convex profile. More precisely, it is given by

$$\kappa_m=-\frac{\partial^2\zeta_m/\partial x^2}{[(\partial\zeta_m/\partial x)^2+1]^{3/2}}. \tag{12}$$

Using Eq. (11), we obtain from Eq. (8)

$$c_{eq}=c_{eq}^0\left\{1+\frac{\Omega}{k_BT}\left[\gamma\kappa_m+\frac{\hat{\mathcal{A}}}{3}\left(\frac{1}{(l+\zeta_{m+1}-\zeta_m)^3}-\frac{1}{(l+\zeta_m-\zeta_{m-1})^3}\right)\right]\right\}. \tag{13}$$

The set of Eqs. (5) and (6), with c_{eq} given by Eq. (13), uniquely determine the concentration fields everywhere on the terraces if the step positions and geometry were given. The present problem is a free boundary problem, where an additional constraint must be evoked to complete the description. This follows from mass conservation equations. Indeed, mass conservation expressed at each step then determines the normal step velocity

$$v_n=\Omega\left[\left(D\frac{\partial c}{\partial n}-\mathbf{n}\cdot\mathbf{q}\right)_+-\left(D\frac{\partial c}{\partial n}-\mathbf{n}\cdot\mathbf{q}\right)_-\right]. \tag{14}$$

The normal velocity can be expressed as a function of the step position as

$$v_n=\frac{V+\partial\zeta/\partial t}{[1+(\partial\zeta/\partial x)^2]^{1/2}}, \tag{15}$$

where V is the drift velocity of a uniform train.

Finally, to complete our description, we must specify the amplitudes of the Langevin forces. A local thermodynamic equilibrium approximation allows us to extend the equilibrium expression of the amplitudes of the Langevin forces to the out of equilibrium situation (see Appendix A). Their correlations take the forms

$$\langle q_{mi}(\mathbf{r},t)q_{m'j}(\mathbf{r}',t')\rangle=2Dc(\mathbf{r},t)\,\delta\delta_{ij}, \tag{16}$$

$$\langle f_m(\mathbf{r},t)f_{m'}(\mathbf{r}',t')\rangle=2\frac{c(\mathbf{r},t)}{\tau}\,\delta, \tag{17}$$

$$\langle\eta_{m\pm}(x,t)\,\eta_{m'\pm}(x',t')\rangle=\frac{2c_\pm(x,t)}{\nu_\pm}\,\delta, \tag{18}$$

where δ is an abbreviation for $\delta(\mathbf{r}-\mathbf{r}')\,\delta(t-t')\,\delta_{m,m'}$ and $c_\pm$ is the adatom concentration close to the step.

Two relevant quantities that characterize the meander $\zeta_m(x,t)$ of the steps in a train are the step roughness w and the interstep correlations $G(p)$. The rms roughness is defined by

$$w^2=\lim_{t_0\to\infty}\frac{1}{t_0}\int_0^{t_0}\frac{1}{N}\sum_{m=0}^{N}\frac{1}{L}\int_0^L dx[\zeta_m(x,t)]^2 \tag{19}$$

in a train of N steps of length L. The definition of the interstep correlations $G(p)$ is

$$G(p)=\lim_{t_0\to\infty}\frac{1}{t_0}\int_0^{t_0}\frac{1}{N}\sum_{m=0}^{N}\frac{1}{L}\int_0^L dx[\zeta_m(x,t)-\zeta_{m+p}(x,t)]^2. \tag{20}$$

One of the first goals will be to determine these quantities and analyze their far reaching consequences. This will constitute a preliminary task before tackling the out-of-equilibrium regime, which is the main purpose of this paper.

B. Green's functions formalism

Equations (5), (6), and (14) completely describe the dynamics of the vicinal surface. We shall first convert them into an integral formulation by means of Green's function techniques. This will allow us to relate the concentration field to its normal derivative at the step. In what follows we use a normalized field $u=\Omega(c-\tau F)$ instead of the concentration c. Equation (5) then becomes

$$\frac{\partial u}{\partial t}=D\nabla^2 u-\frac{u}{\tau}+\Omega(f-\boldsymbol{\nabla}\cdot\mathbf{q}). \tag{21}$$

We obtain two integral equations for $\mathbf{r}=\zeta_m+ml$ and $\mathbf{r}=\zeta_{m+1}+(m+1)l$ (any quantity to be evaluated at ζ_m will be indicated by the symbol $\pm$, which means on the right- and left-hand sides, respectively). Their derivation is detailed in Appendix B. We find

$$\begin{aligned}&\int_{-\infty}^{t}dt'\Bigg[\tau\int_{-\infty}^{\infty}dx'(V+\dot{\zeta}')u'G\\&\quad+D\tau\int d\Gamma_s'\left(G\frac{\partial u'}{\partial n'}-u'\frac{\partial G}{\partial n'}\right)\Bigg]_{z'=ml+\zeta_m'}^{z'=(m+1)l+\zeta_{m+1}'}\\&\quad+\Omega\tau\int_{-\infty}^{t}dt'\int_{-\infty}^{\infty}dx'\int_{ml+\zeta_m}^{(m+1)l+\zeta_{m+1}}dz'(f'-\boldsymbol{\nabla}'\cdot\mathbf{q}')G\\&\quad=\frac{1}{2}u(\mathbf{r},t)\big|_{\pm},\end{aligned} \tag{22}$$

where $G(\mathbf{r}-\mathbf{r}',t-t')$ is the free propagator and is given by (see Appendix B)

$$\begin{aligned}G(\mathbf{r}-\mathbf{r}',t-t')=\frac{\mathbf{Y}(t-t')}{(t-t')4\pi D\tau}\exp\Bigg[-\frac{t-t'}{\tau}\\-\frac{(x-x')^2+[z-z'+V(t-t')]^2}{4D(t-t')}\Bigg],\end{aligned} \tag{23}$$

where $\mathbf{Y}$ is the Heaviside function. The quantities indicated by prime are understood to depend on $\mathbf{r}'$ and t' (note that because G is a function of both variables, we do not specify the variables). We can express the normal derivative of u as a function of u. Indeed, using Eq. (6) with c_{eq} given by Eq. (13), we obtain

$$\begin{aligned}\left.\frac{\partial u}{\partial n}\right|_{\pm}&=\mathbf{n}\cdot\mathbf{q}\frac{\Omega}{D}\pm\frac{1}{d_{\pm}}(u_{\pm}+\sigma\Omega c_{eq}^0+\Omega\eta_{\pm})\\&\quad\mp\frac{1}{d_{\pm}}\Bigg[\Gamma\kappa+\frac{A}{3}\Bigg(\frac{1}{(l+\zeta_{m+1}-\zeta_m)^3}\\&\quad-\frac{1}{(l+\zeta_m-\zeta_{m-1})^3}\Bigg)\Bigg],\end{aligned} \tag{24}$$

where $\sigma=\tau F/c_{eq}^0-1$ is the supersaturation, $d_{\pm}=D/\nu\pm$ are lengths that we shall refer to as the ES lengths $\Gamma=\Omega^2 c_{eq}^0\gamma/k_BT$, and $A=\Omega^2 c_{eq}^0(\hat{\mathcal{A}}/k_BT)$. The length d_t can be thought of as the mean excursion length of an atom before it sticks to a step. If N is the number of steps, Eq. (22) corresponds to $2N$ equations, while we have $3N$ unknowns in total, $u_{m\pm}$ and ζ_m. However, with the help of Eq. (24), Eq. (14) provides the normal velocity of a step as a function of the concentration fields u. We then have N other equations. The problem is well posed. These equations are highly nonlinear and nonlocal in space and time. The nonlinearities originate from the boundary conditions (6) and (14), as well as from the free boundary character. The latter source of nonlinearity was hidden in the original equations. Use of Green's functions techniques makes it transparent. In this context this type of technique was used earlier.[13,14] The nonlocal effects are due to the self-interaction of a step (that is, even an isolated step is governed by nonlocal dynamics) and the mutual step-step interaction via the diffusion field and elastic coupling. We shall concentrate here on a linear regime (small variations of the meander), which is valid at equilibrium and for a weakly out-of-equilibrium regime. A nonlinear analysis is discussed in the following paper.

III. LINEAR ANALYSIS

We study regression of fluctuations in the linear regime. Since in the linear regime Fourier modes do not couple, it suffices to consider one Fourier component. In an infinite train of steps, the Fourier transform of ζ (this definition holds for any quantity) will be defined as

$$\zeta_{\omega k\Phi}=\sum_{m=-\infty}^{m=+\infty}\int_{-\infty}^{+\infty}dt'\int_{-\infty}^{+\infty}dx\,\zeta_m(x,t)e^{-i(\omega t+kx+m\Phi)}, \tag{25}$$

where ω, k, and Φ are the Fourier conjugate variables of t, x, and m. For ζ we retain the linear terms only, while the normalized concentration field u is developed in the following way:

$$u=u_0+u_1+b. \tag{26}$$

Here u_0 is the zeroth-order field (listed in Appendix B 2), u_1 is a small deviation corresponding to the deterministic part, and b is a term standing for the stochastic part. When plugging Eq. (26) into the integral equation (22) and linearizing in u_1 and ζ we obtain a zeroth-order equation (fixing u_0) and a linear contribution relating the u_1's to ζ_m's and a relation determining the fluctuating part b as a function of the already introduced Langevin forces. Use of Fourier transforms allows us to diagonalize these equations and we can eliminate $u_{1\omega k\Phi}$ to the advantage of $\zeta_{\omega k\Phi}$. Finally, using Eq. (14), we obtain an inhomogeneous expression for $\zeta_{\omega k\Phi}$, which takes the form

$$\zeta_{\omega k\Phi}=\chi_{\omega k\Phi}\beta_{\omega k\Phi}, \tag{27}$$

where χ is the linear susceptibility of the steps and β is a noise resulting from the Langevin forces introduced above. Their general expressions is given in Appendix B. We would like to mention that this result involves very lengthy algebra, which is avoided here. Note that in real space, Eq. (27) represents a *nonlocal* Langevin equation with a *colored* noise in both space and time.

We can now evaluate the expression of the roughness w of the step. From the very definition of the roughness [Eq. (19)] we have

$$w^2=\int\frac{dk}{2\pi}\int\frac{d\Phi}{2\pi}\int\frac{d\omega}{2\pi}\langle|\zeta_{\omega k\Phi}|^2\rangle = \int\frac{dk}{2\pi}\int\frac{d\Phi}{2\pi}\int\frac{d\omega}{2\pi}\langle|\beta_{\omega k\Phi}|^2\rangle|\chi_{\omega k\Phi}|^2. \tag{28}$$

The interstep correlation function takes the form $G(p)$,

$$G(p)=\langle[\zeta_m(x,t)-\zeta_{m+p}(x,t)]^2\rangle = 2\int\frac{dk}{2\pi}\int\frac{d\Phi}{2\pi}\int\frac{d\omega}{2\pi}\langle|\beta_{\omega k\Phi}|^2\rangle \times|\chi_{\omega k\Phi}|^2[1-\cos(p\Phi)]. \tag{29}$$

Before treating the out-of-equilibrium situation, we shall first study their equilibrium properties.

IV. EQUILIBRIUM THEORY REVISITED

A. Equilibrium static spectrum

In this section we discuss some immediate results concerning equilibrium. This task constitutes an interesting check of the formalism. We shall limit ourselves in this discussion to the static features. An extensive analysis including dynamical evolution of fluctuations at equilibrium is presented elsewhere.[16] We shall exploit first the general linear relation (27) at equilibrium and in the quasistatic approximation (see later) ($\omega\ll Dk^2$). Using the expressions given in Appendix B for β and χ, we get

$$\langle\zeta_{\omega k\Phi}\zeta_{-\omega-k-\Phi}\rangle=\frac{\langle\beta_{\omega k\Phi}\beta_{-\omega-k-\Phi}\rangle}{\chi^{-1}_{\omega k\Phi}\chi^{-1}_{-\omega-k-\Phi}}=\frac{2\Omega^2c^0_{eq}\dfrac{\Lambda_k}{\mathcal{D}}D\{f_k+2[1-\cos(\Phi)]\}}{\omega^2+\left[\left(\Gamma k^2+2\,\dfrac{\hat{\mathcal{A}}}{4}[1-\cos(\Phi)]\right)\dfrac{\Lambda_k}{\mathcal{D}}D\{f_k+2[1-\cos(\Phi)]\}\right]^2}, \tag{30}$$

where we have defined

$$\Lambda_k=\sqrt{k^2+\frac{1}{x_s^2}}, \tag{31}$$

$$f_k=2[\cosh(\Lambda_k l)-1]+\Lambda_k(d_++d_-)\sinh(\Lambda_k l). \tag{32}$$

The static spectrum of the meander is found by integrating Eq. (30) with respect to ω. We find

$$\langle\zeta_{k\Phi}\zeta_{-k-\Phi}\rangle=\frac{k_BT}{\gamma k^2+2\,\dfrac{\hat{\mathcal{A}}}{l^4}[1-\cos(\Phi)]}. \tag{33}$$

We recall that in real space Eq. (27) is nonlocal and the noise is colored in a complicated manner. Nevertheless, the static spectrum takes the simple form given by Eq. (33) in all situations. This is a result of the fact that the dynamical equations can be derived from a Lyapunov functional. We can alternatively obtain this result from equipartition of the step energy on the Fourier modes.

B. Isolated step

Before considering the case of a train of steps, let us first recall the well-known expression of the roughness for an isolated step. The associated energy is $\mathcal{E}=(\gamma/2)\int_0^L dz(\partial\zeta/\partial x)^2$. The roughness reads[2]

$$w_s^2=\sum_{k=2\pi/L}^{\infty}\frac{k_BT}{L\gamma k^2}=\frac{k_BT}{12\gamma}L, \tag{34}$$

where L is the step length (Fig. 2). This is a well-known result. Note the analogy with one-dimensional Brownian motion, where L represents time.

C. Entropic confining: A step between two walls

The case where a step fluctuates at equilibrium between two straight and motionless steps (the Gruber-Mullins case[3])

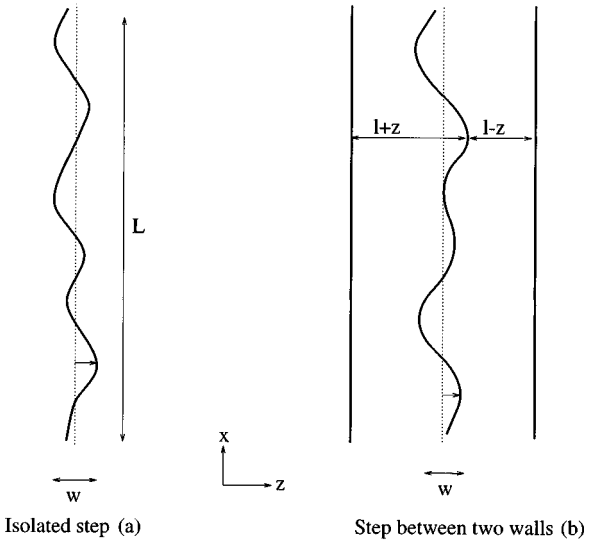

FIG. 2. At equilibrium, the roughness of an isolated step (a) is proportional to the square root of the length L of the step $w\sim L^{1/2}$. (b) A step fluctuates between two straight and motionless steps. The steps interact via an elastic repulsion potential $U\sim l^{-2}$, where l is the interstep distance. Then $w\sim l$.

(Fig. 2) has been studied by Bartelt *et al.*[5] Their expression of the roughness is recovered here. Our model is easily modified to treat this case. For that purpose we set $\zeta_{m+1}=\zeta_{m-1}=0$. There is no more translational invariance with respect to the direction z and no more ϕ variable in Fourier space. Following the same line as in Sec. IV A [in particular in Eq.(33), we set $\cos(\Phi)=0$, which is equivalent to setting $\zeta_{m+1}=\zeta_{m-1}=0$], the following static spectrum is obtained:

$$\langle \zeta_{k\Phi}\zeta_{-k-\Phi}\rangle = \frac{k_BT}{\gamma k^2+2\,\dfrac{\hat{\mathcal{A}}}{l^4}}. \tag{35}$$

Using Eq. (28), the roughness is then easily calculated

$$w_s = l\left(\frac{(k_BT)^2}{8\gamma\hat{\mathcal{A}}}\right)^{1/4}, \tag{36}$$

in agreement with Bartelt *et al.*[5]

D. Step roughness on a vicinal surface

If all the steps meander, the step roughness can be calculated from expression (33). The divergence of the static spectrum at $\Phi=0$ and $k=0$ is interpreted as a Goldstone mode related to the translational invariance of an infinite train of steps. This leads to a logarithmic divergence of the meander with the size of the train. This is easily seen by analyzing the behavior of the static spectrum (33) in the long-wavelength limit $(k,\Phi\to 0)$, where the divergence occurs. A finite number of steps N or a finite length of the steps L introduces a cutoff $\Phi_0=2\pi/N$ or $k_0=2\pi/L$. The behavior of the roughness is controlled by the largest term of the denominator of Eq. (33) when $\Phi=\Phi_0$ and $k=k_0$. There are two possible cases. (i) The line tension term dominates. This entails that

$$\gamma k_0^2 > \frac{\hat{\mathcal{A}}}{l^4}\Phi_0^2. \tag{37}$$

Taking $\hat{\mathcal{A}}/\gamma\sim a^2$, we find the condition

$$L < \frac{l^2}{a}N. \tag{38}$$

Even in a small bunch of $N=10$ steps, with an interstep distance $l=10^2$ atomic lengths, this condition is fulfilled for $L<10^5$ atomic lengths. We therefore expect condition (38) to be safely fulfilled in real systems. The roughness takes the following form in this case:

$$w_s \simeq \frac{l}{\sqrt{2\pi}}\left(\frac{(k_BT)^2}{\gamma\hat{\mathcal{A}}}\right)^{1/4}[\ln(L\tilde{a}/l^2)]^{1/2}, \tag{39}$$

where $\tilde{a}\equiv(1/\pi)(\hat{\mathcal{A}}/\gamma)^{1/2}$, which has the dimension of a length and is of the order of an atomic length. The roughness is not linear in l. This is to be contrasted with Eq. (36), where the neighboring steps are frozen. While an experimental study to detect the logarithmic divergence is challenging, this is an interesting result in itself on the conceptual level. (ii) The second case corresponds to a situation where the elastic effect becomes important. This occurs when reducing the interstep distance. For example, for a small interstep distance, a small number of steps, and a large enough lateral step extent (for example, $N=10$, $l=10$, and $L=10^5$) condition (38) is not verified. Then the step roughness reads

$$w_s \simeq \frac{l}{\sqrt{2\pi}}\left(\frac{(k_BT)^2}{\gamma\hat{\mathcal{A}}}\right)^{1/4}\left(\ln\left[\frac{2N}{\pi}\right]\right)^{1/2}. \tag{40}$$

In this case w is linear in l and the cutoff follows here from a finite number of steps.

E. Interstep correlations and terrace width fluctuations

At equilibrium, the step correlations are predicted to diverge logarithmically with the distance between the steps[2,17] above the roughening temperature. The calculation of the correlations is straightforward from Eq. (29). We find

$$G_S(p)=\langle(\zeta_m-\zeta_{m+p})^2\rangle=\frac{1}{2}\,\frac{k_BTl^2}{\sqrt{\gamma\hat{\mathcal{A}}}}\,\alpha_p, \tag{41}$$

where

$$\alpha_p=\sqrt{2}\int\frac{d\Phi}{2\pi}\,\frac{(1-\cos[p\Phi])}{(1-\cos[\Phi])^{1/2}}. \tag{42}$$

The logarithmic divergence of α_p is shown in Appendix C. Experimentally, these correlations have been studied by Heyraud *et al.*[18] as a function of p. The comparison of our expression (41) to their experimental values allows us to deduce the product $\gamma\hat{\mathcal{A}}$. If we take their experimental value obtained for γ [from the study of fluctuations of an isolated step, using expression (34)], $\gamma=1.1\times10^{-10}$ J m^{-1} at $T=1173$ K,[19] we find $\hat{\mathcal{A}}\simeq1\times10^{-28}$ J m.

In another paper Alfonso *et al.*[19] have investigated the statistics of the terrace width fluctuations. This quantity is given here by Eq. (41) with $p=1$:

$$G_S(1)=\frac{2}{\pi}\,\frac{k_BTl^2}{\sqrt{\gamma\hat{\mathcal{A}}}}. \tag{43}$$

Using the experimental results of Alfonso *et al.*,[19] we find $\hat{\mathcal{A}}\simeq1\times10^{-28}$ J m. This estimate is quite consistent with the one given above by analyzing the function $G(p)$. However the absolute value provided by Alfonso *et al.*[19] is $\hat{\mathcal{A}}\simeq3\times10^{-29}$ J m (actually, they used another definition of $\hat{\mathcal{A}}$ than what we use here; their definition is six times smaller than ours). This is about three times smaller than what we gave above. This discrepancy comes from the fact that they used Eq. (36) as an approximation of the terrace width fluctuations[5] and not Eq. (43) as it should be. Inspection of Eqs. (36) and (43) reveals that the value of $\hat{\mathcal{A}}$ extracted from Eq. (43) is bigger than that obtained from Eq. (36) by a factor $32/\pi^2\sim3$. This explains the discrepancy.

V. OUT OF EQUILIBRIUM

A. General features

During growth, we expect two qualitatively different phenomena induced by the Ehrlich-Schwœbel effect. First, the

train of steps is stabilized against step bunching and/or step crossing. Figure 3 summarizes this effect. Second, a straight step is morphologically unstable when the supersaturation $\sigma=\tau F/c_{eq}^0-1$ exceeds a threshold value denoted below by σ_{BZ}. This was shown by Bales and Zangwill[8] for a train of synchronized steps ($\Phi=0$ in our model). This is easily understood for an isolated step in the presence of desorption (see Fig. 4). Far from the step, the concentration is constant and equal to $c_\infty=\tau F$. A fluctuation of the position of the step leads to an increase of the concentration gradient in front of it (very much like in electrostatics when high curvatures on a conductor cause an increase of the electric field) and therefore to an increase of the incoming adatom flux on the lower terrace. If there is no attachment from the upper terrace or if the jump over the ES barrier is not instantaneous, the perturbation grows and the step is unstable. Moreover, fluctuations associated with shot noise, conserved noise, and attachment/detachment noise at the steps roughen the steps. The step meander thus stems from a cooperative effect between stochastic and deterministic effects.

If the diffusion process is fast enough, the time derivative in Eq. (5) can be neglected. This is the quasistatic approximation. This means that the diffusion field adapts itself instantaneously to the step motion. In other words, the diffusion time for an adatom to find a coordination site on the step is typically of the order $t_1\sim l^2/D$. This time is to be compared with the advance time of the step by an amount of the order of an atomic distance. This is approximately given by $t_2\sim\Omega^{1/2}/\Omega F l$. The quasistatic approximation is valid as long as $t_1\gg t_2$. For example, for Si(111) at $T=1000$ K, $D/\Omega\sim10^8$ s^{-1}, $\Omega F\sim1$ s^{-1}, $l\sim10^2$ atomic lengths, and therefore $t_1=10^{-4}$ s$\ll t_2=10^{-2}$. This means that for not too large terrace widths, sufficiently large diffusion constants, and reasonably small fluxes, this approximation is valid. These conditions coincide with the ones needed to prevent island nucleation on the terraces, a phenomenon that is not considered here.

We shall first consider the case where desorption is not negligible on length and time scales of interest. We will return later to the opposite situation.

B. Growth with adatom desorption

In this section we shall first consider the situation of weak enough fluxes in order to prevent the Bales-Zangwill instability. It will appear that the elastic repulsion is immediately overcome by the diffusive repulsion. The meander of a step at equilibrium is caused by statistical fluctuations and limited by elastic interactions [see Eq. 36)]. Here the meander will be fixed by the diffusive repulsion.

The calculation can be made in the general case, but we shall limit ourselves to the case where desorption is small (but nonzero). We expect this limit to represent many situations in MBE growth. Moreover, we shall distinguish between a small and a large ES effect. On the other hand, the evolution equation is nonlocal in space. We shall discuss below the limit of long wavelengths, that is, we consider the situation where $k\lambda_0\ll1$, with $\lambda_0=\max(x_s,l)$. In this limit dynamics become local.

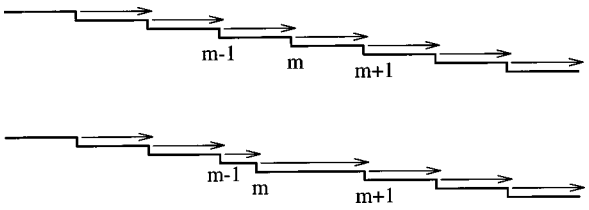

FIG. 3. The Schwœbel effect leads to a repulsion between steps during growth. For the sake of simplicity, we consider a one-sided model (strong ES effect): The adatom coming from the upper terrace cannot attach to a step ($\nu_-=0$). If desorption is small, the velocity of a step V is approximately proportional to the number of adatoms that land on the lower terrace. This number is proportional to the terrace width l. Hence V is proportional to the width of the lower terrace. We consider a train of steps initially separated by l. Now let the mth step fluctuate from its original position in the $-z$ direction. Its velocity will increase and that of the $(m-1)$th step will decrease. The train of steps is stable.

Small ES effect and weak desorption.

By a weak ES effect we mean $d_+,d_-\ll l$ and a weak desorption $x_s\gg l$. The adatoms coming from the lower terrace stick more easily to the step. We shall set below $d_+=0$ (attachment is instantaneous) for the sake of simplicity. Using the expression of the response function χ given in Appendix B, we find to leading order in k a polynomial of order 2. Realizing that $\cos(\Phi)$ (entering the expansion of χ) produces $\zeta_{m-1}+\zeta_{m+1}$, we can immediately write the evolution equation in real space as

$$\frac{\partial\zeta_m}{\partial t}=-\left[\frac{A}{l^3}\left(\frac{1}{\tau}+\frac{D}{l^2}\Theta_m\right)+\frac{\Omega c_{eq}^0}{\tau}\sigma\left(\frac{d_-}{l}\right)^2\right]\Theta_m\zeta_m+\frac{l d_-}{2\tau}\left(\frac{2\Gamma}{d_-}-\Omega c_{eq}^0\sigma\right)\frac{\partial^2\zeta_m}{\partial x^2}+\left[\frac{D}{l}\left(\Gamma+\frac{A}{l^2}\right)-\frac{\Omega c_{eq}^0}{\tau}\sigma\frac{d_-^2}{6}\right]\Theta_m\frac{\partial^2\zeta_m}{\partial x^2}+\frac{\Omega c_{eq}^0}{2\tau}\sigma\left[\zeta_{m+1}-\zeta_{m-1}+\frac{l^2}{6}\left(\frac{\partial^2\zeta_{m+1}}{\partial x^2}-\frac{\partial^2\zeta_{m-1}}{\partial x^2}\right)\right]+\beta_m,\tag{44}$$

where we have defined the operator Θ that acts on a function g_n as $\Theta_n g_n=2g_n-g_{n+1}-g_{n-1}$. The amplitude of the resulting Langevin force is found in this limit to obey [using the definition (27) and the expression of β given in Appendix B expanded according to the regime we are interested in]

$$\langle\beta_m(\mathbf{r},t)\beta_{m'}(\mathbf{r}',t')\rangle=2\Omega^2c_{eq}^0\frac{D}{l}\left(\frac{l^2}{x_s^2}+\Theta_{m'}\right)\times\delta_{m,m'}\delta(\mathbf{r}-\mathbf{r}')\,\delta(t-t').\tag{45}$$

Using Eq. (27) in this limit, the roughness is easily calculated:

$$w=\Omega^{1/2}\left(\frac{x_s^2 l}{2(\Gamma/\Omega c_{eq}^0)\sigma d_-^2}\right)^{1/4}.\tag{46}$$

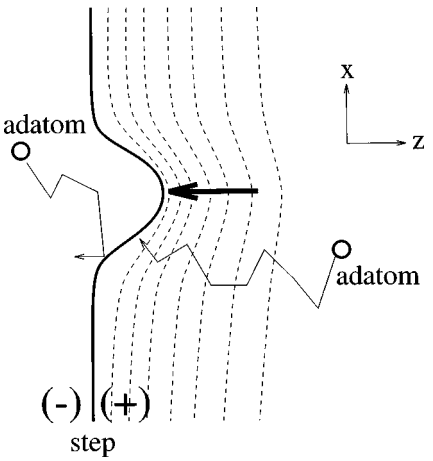

FIG. 4. An adatom diffusing on the lower terrace (+) has a higher probability to stick on a protuberance of the step. The incoming adatom flux is therefore higher on the protuberance. The dashed lines are isoconcentration lines. If the ES effect is important (−), the protuberence increases. Diffusion destabilizes the steps during growth. This effect overcomes the smoothening due to the step stiffness when the supersaturation σ exceeds a threshold value σ_{BZ}.

Making use of the definition of $\sigma \sim \tau F/c_{eq}^0$ (when desorption is negligible), $x_s^2 = D\tau$, and $\Gamma = \Omega^2 c_{eq}^0 \gamma / k_B T$, we recover Eq. (4). We see here the effect of the diffusive repulsion: the step must smoothen as the incoming flux increases, $w \sim \sigma^{-1/4}$. We have seen in Eq. (36) that the elastic interaction (which is taken as $1/l^2$) produces a meander $\sim l$. In order to produce a meander $\sim l^{1/4}$, in an energetic picture, the effective energy of the diffusive repulsion must behave as

$$\mathcal{E} \sim l \ln[l]. \tag{47}$$

This dynamical smoothening leads to a reduction of the terrace width fluctuations. This is measured by the ratio

$$R = \frac{G_D(1)}{G_S(1)} = \frac{\pi}{\sqrt{2}} \frac{x_s}{d_- l^{3/2}} \left(\frac{A/\Omega c_{eq}^0}{\sigma} \right)^{1/2}. \tag{48}$$

For Si(111), at a high enough temperature, we expect $d_+ \sim 0$, $d_- \sim 10^2$, $A/\Omega c_{eq}^0 \sim 1$, and $x_s \sim 10^4$, where lengths are measured in atomic units. For $l \sim 10^3$ and $\sigma \sim 10^{-2}$, we find $R \sim 10^{-1}$.

Studying the terrace width fluctuations for straight steps in the $F/D \to 0$ and $\tau \to 0$ limit, in a Monte Carlo simulation Krug and Schimschak[20] found that the terrace with fluctuations should behave like $l^{1/2}$, compared to $l^{1/4}$ in our model. We give in the next section an argument for their finding.

C. No desorption and a strong ES effect

If desorption is completely negligible, that is to say, if the diffusion length x_s is much bigger than all scales of interests (l, $d_\pm$, and the wave vector k), the straight step is in principle unstable however small the incoming flux is. It is shown below that, though this situation is more unstable than that corresponding to the case with desorption, a finite flux is required to induce the instability. This is due to the fact that the system always exhibits finite size effects.

Let us first discuss the situation of a translationally invariant train. We concentrate on the situation where the ES effect is very large, so that the probability for an adatom to descend a step is very small. This is expected to be the case for small enough temperatures. Formally, this amounts to letting $d_- \to \infty$. This is the so-called one-sided model, where step dynamics are due to the adatoms coming from one side, namely, the lower one.

If desorption is negligible and the ES effect is large, we expect that the step dynamics can be described by that of a conserved quantity. Indeed, this limit prohibits the terrace from exchanging mass with either the atmosphere or adjacent terraces. Following the same strategy as in Sec. V B (that is, expanding χ to leading order in k, here the expansion is valid for $kl \ll 1$), we obtain in real space

$$\begin{aligned} \frac{\partial \zeta_m}{\partial t} &= \Omega F(\zeta_{m+1} - \zeta_m) \\ &+ \frac{\partial^2}{\partial x^2} \left\{ -\Omega F \frac{l^2}{2}(2\zeta_m - \zeta_{m+1}) \right. \\ &- \Omega F \frac{l^4}{8} \left(\frac{4}{3} \frac{\partial^2 \zeta_m}{\partial x^2} - \frac{1}{3} \frac{\partial^2 \zeta_{m+1}}{\partial x^2} \right) \\ &\left. + Dl \left[-\Gamma \frac{\partial^2 \zeta_m}{\partial x^2} + \frac{A}{l^4} \left(1 - \frac{l^2}{3} \frac{\partial^2}{\partial x^2} \right) \Theta_m \zeta_m \right] + \right\} \\ &+ H_m, \end{aligned} \tag{49}$$

where the resulting noise H_m satisfies the correlation law

$$\langle H_m(\mathbf{r},t) H_{m'}(\mathbf{r}',t') \rangle = 2\Omega^2 D c_{eq}^0 l \frac{\partial^2 \delta}{\partial x^2}. \tag{50}$$

The first term tells us that the drift velocity of a step in a uniform train is proportional to the forward terrace width. The other term corresponds to dynamics of a conserved quantity $\partial \zeta / \partial t = -\partial J / \partial x$. At equilibrium, that is, for $F = 0$, Eq. (49) is of fourth order in space. This is symptomatic of an effective diffusion along the steps: Adatoms make large excursions on the terrace (without escaping it, because desorption is absent at the scale of the terrace and the ES effect is strong so that no mass exchange between terrace occurs) before they stick to the upper step. This is a pure one-dimensional diffusion with an effective diffusivity $\sim Dl$.

As is seen from Eq. (49), the absence of desorption immediately lead to an instability signaled by the negative sign of the first term in curly brackets ($-Fl^2 \zeta_m$). Except when finite size effects are important (see Sec. V D), a deterministic instability is present and a special treatment of the roughness is necessary (see later). It is however instructive to see why Krug and Schimschak's[20] study based on Monte Carlo simulations has led to a terrace width fluctuation that increases as $l^{1/2}$. This result follows directly from the fact that if meandering is forbidden together with desorption and in the presence of a strong ES effect (as is assumed in their work), then the step dynamics is governed by Eq. (49) where all derivatives with respect to x are absent,

$$\frac{\partial \zeta_m}{\partial t} = \Omega F(\zeta_{m+1} - \zeta_m) + f(t), \tag{51}$$

where we have added a different source of noise related to the fully nonequilibrium shot noise (not present in our original formulation assuming a local equilibrium). This shot noise is well known to have a variance $\langle f(t)f(t')\rangle \sim Fl\delta(t-t')$ (the factor l comes simply from the fact the velocity of the step is related to that of the surface by the tilt angle, which is proportional to $1/l$). Then a simple calculation (after Fourier transforming in Φ and ω and integrating over the two variables) leads to $w \sim l^{1/2}$, which is the result of Krug and Schimschak. Introducing such a formulation of noise in our full study is of course feasible, but will constitute the subject of future work.

D. Higher fluxes: A deterministic instability

At higher fluxes, the supersaturation reaches the morphological instability threshold. Starting from the general dispersion relation given in Appendix B, we can show that the bifurcation occurs for $k=0$ and $\Phi=0$, that is to say, this is the most dangerous mode (which is due to the existence of a Goldstone mode). Then it is sufficient to expand the dispersion relation for small k to determine the threshold value. The leading term behaves as k^2 and setting the prefactor to zero provides us with the general expression for the threshold condition. The calculation is straightforward and the result can be written as

$$\sigma_{BZ} = \frac{2\Gamma}{\Omega c_{eq}^0} \frac{\mathcal{D}_0}{(d_- - d_+)\sinh(l/x_s)}, \tag{52}$$

where $\mathcal{D}_0$ is defined in Appendix B and $\Gamma = \Omega^2 c_{eq}^0 \gamma / k_B T$. In the case of instantaneous kinetics from the lower terrace ($d_+ = 0$), this condition reduces to

$$\sigma_{BZ} = 2\Gamma/\Omega c_{eq}^0 [1/d_- + 1/x_s \coth(l/x_s)] \simeq \frac{2\Gamma/\Omega c_{eq}^0}{\min(d_-, l, x_s)}. \tag{53}$$

We assume in writing the second form that one length is significantly smaller than the others. This expression is interesting since it shows that only the smallest length is relevant for the instability. The physical reason is the following. For example, if $l \ll x_s, d_-$, this means that all adatoms on the terrace of width l will potentially contribute to the instability. The threshold value for the supersaturation is fixed by Γ/l. Conversely, if $x_s \ll l, d_-$, then only those adatoms that reach the step will cause the instability, while several of those that were originally available on the terrace will regain the atmosphere before attaining the step; desorption plays the role of a short circuit against the instability. Finally, if d_- is the smallest length, the adatoms will at most attempt an excursion of order d_- before they attach to a step.

One of the most important features during MBE is that the steps are morphologically unstable above a critical value of deposition flux. This is a deterministic instability and by its very definition any fluctuation at the threshold will blow up rapidly in the course of time. This is signaled by the divergence of the response function χ. We expect, therefore, the meander to exhibit a divergence as well. The general discussion for a train is presented in Appendix C. It is interesting first to recall the results for an isolated step. The static spectrum of an isolated step is of the form [see Eq. (C1) in Appendix C, where we set $l=\infty$]

$$\langle \zeta_k \zeta_{-k} \rangle \sim \frac{1}{\epsilon k^2}, \tag{54}$$

where $\epsilon = 1 - \sigma/\sigma_{BZ}$. The roughness then reads[21]

$$w \sim \left(\int_{2\pi/L}^{+\infty} \frac{dk}{2\pi} \frac{1}{\epsilon k^2} \right)^{1/2} \sim \frac{L^{1/2}}{\epsilon^{1/2}}. \tag{55}$$

The meander of an isolated step diverges like $1/\epsilon^{1/2}$, in agreement with Refs. 10 and 21. The exponent is different in the case of a train. Indeed, in that case the phase Φ intervenes in the static spectrum. The part of this static spectrum that leads to the divergence of the roughness has the form (see Appendix C)

$$\langle \zeta_{k,\Phi} \zeta_{-k,-\Phi} \rangle \sim \frac{1}{\epsilon k^2 + [1 - \cos(\Phi)] a(k)}, \tag{56}$$

where $a(k)$ is a complicated expression resulting from interactions between steps (for details see Appendix C). This leads to a different exponent. Indeed, the roughness is given by

$$w \sim \left(\int_{2\pi/L}^{+\infty} \frac{dk}{2\pi} \int_0^{2\pi} \frac{d\Phi}{2\pi} \frac{1}{\epsilon k^2 + [1 - \cos(\Phi)] a(k)} \right)^{1/2}. \tag{57}$$

Since $a(k) \neq 0$ for $k \to 0$ (this simply means that there are interactions between straight steps),

$$w \sim \left(\int_{2\pi/L}^{+\infty} \frac{dk}{2\pi} \frac{1}{(\epsilon k^2)^{1/2} a(k)^{1/2}} \right)^{1/2} \sim \frac{[\ln(L)]^{1/2}}{\epsilon^{1/4}}. \tag{58}$$

The change between Eqs. (55) and (58) is the result of the repulsive interaction of each step with its neighbors. In the train of steps the roughness divergence with the size of the system is logarithmic instead of being algebraic. Furthermore, the divergence caused by the morphological instability is also weakened ($w \sim \epsilon^{-1/4}$ instead of $w \sim \epsilon^{-1/2}$). The qualitative behavior of w as a function of the incoming flux is displayed in Fig. 5.

In the case of weak evaporation $l \ll x_s$ and far from this threshold ($\sigma \ll \sigma_{BZ}$), the terrace width fluctuations $G_D(1)$ are simply related to the step roughness by $G_D(1) \simeq 2w^2$ (see Appendix C). Actually, we always have the inequality $G_D(1) < 2w^2$ at equilibrium. Nevertheless, $G_D(1)$ does not diverge when the supersaturation increases and reaches σ_{BZ}.

For p not too large [$p < x_s^2/(l^2 + l d_+ + l d_-)$], $G_D(p)$ exhibits a linear dependence on p,

$$G_D(p) \simeq G_D(1) \left[1 + p \frac{l(l + d_+ + d_-)}{2x_s^2} \left(1 - \frac{1}{2} \frac{1 - \sigma/\sigma_{BZ}}{1 + \sigma/\sigma_0} \right) \right], \tag{59}$$

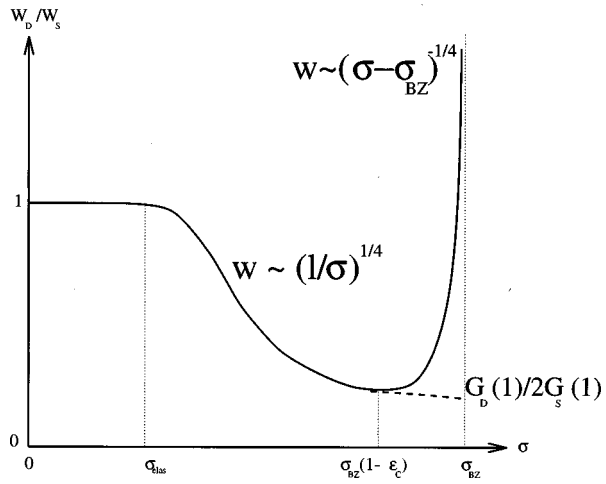

FIG. 5. Step roughness as a function of the supersaturation $\sigma = \tau F/c_{eq} - 1$ in the case of a weak Ehrlich-Schwœbel effect. When the supersaturation increases, the roughness goes through different regimes. First, when $\sigma < \sigma_{elas}$ the supersaturation is constant. If $\sigma_{elas} < \sigma < \sigma_{BZ}(1-\epsilon_c)$, the diffusive repulsion overcomes the elastic repulsion and the roughness decreases $w_D \sim (l/\sigma)^{1/4}$. When $\sigma_{BZ}(1-\epsilon_c) < \sigma < \sigma_{BZ}$, the roughness diverges $w_D \sim (\sigma - \sigma_{BZ})^{-1/4}$. The terrace width fluctuation $G_D(1)$ remains finite in this region. When $\sigma > \sigma_{BZ}$, the steps are morphologically unstable and a nonlinear analysis is necessary.

where σ_0 is defined in Appendix C. If $p \gg x_s^2/(l^2 + l d_+ + l d_-)$, $G_D(p) \sim \ln(p)$. At large enough scales and whether or not we are at equilibrium, the correlations together with the roughness diverge logarithmically with the size of the system,[2] whereas the interstep correlation function $G_D(p)$ remains finite at the morphological instability threshold $\sigma = \sigma_{BZ}$ for a given value of p.

In principle, in the absence of desorption and as shown by the term $\sim F$ in Eq. (49), the steps are always unstable. We show now that finite size effects introduce always a restriction on a minimal value. For that purpose we consider the dispersion relation (written in Appendix B) in the limit of *no desorption* and in the case of a finite train of steps. A finite number of steps N introduces a phase cutoff $\Phi_0 = 2\pi/N$. Taking the $k=0$ limit, we obtain that the diffusive repulsion overcomes the elastic repulsion if $\Omega F \gg \Omega F_{elas} = 2\Phi_0^2 D(A/l^4)(l + d_- + d_+)/(d_-^2 - d_+^2)$. We now consider meandering steps ($k \neq 0$). The main contribution to the meander comes from the most dangerous modes, i.e., the modes with the smallest value of Φ. For these modes $\Phi \sim \Phi_0 \ll 1$. We write the real part of the dispersion relation resulting from Eq. (B11) to leading order in k and Φ,

$$\mathrm{Re}[i\omega(k,\Phi)] = -\frac{\Phi^2}{2}\Omega F \frac{d_-^2 - d_+^2}{(l + d_+ + d_-)^2} + \left(-D\Phi^2\Gamma + \Omega F \frac{l^2}{2}(d_+ - d_+) \right) \frac{k^2}{(l + d_+ + d_-)}. \quad (60)$$

This is stable against meandering if the prefactor of k^2 is negative. Note that because we are interested in a situation where the leading term in k is stabilizing, there is no need to go beyond that order. Since the most unstable mode is the mode $\Phi = \Phi_0$, stability is achieved under the condition

$$\Omega F \ll \Omega F_{BZ} = 2\Phi_0^2 D\Gamma/(d_+ - d_-)l^2. \quad (61)$$

The step roughness is then well defined. Now we use Eqs. (28) and (B13) in the no-desorption limit ($\tau \to \infty$) to calculate the roughness

$$w = \left(\frac{\Omega D c_{eq} k_B T (l + d_+ + d_-)}{2\gamma F (d_-^2 - d_+^2)} \right)^{1/4}, \quad (62)$$

which leads to an expression similar to Eq. (46), in the case of a weak ES effect ($d_+, d_- \ll l$). In a train of $N = 100$ steps on a Si(111) surface, with $d_+ = 0$, $d_- = 10^2$, $l = 10^2$, $\Gamma/\Omega c_{eq}^0 = 1$, and $D c_{eq}^0 = 10^8$, we find $\Omega F_{BZ} = 1\ \mathrm{s}^{-1}$ and $\Omega F_{elas} = 10^{-4}\ \mathrm{s}^{-1}$. Since Φ_0 is inversely proportional to N, the condition (61) is violated for large enough trains, so that the instability manifests itself without a threshold.

If there is in fact a weak desorption, the cutoff $\Phi_0 = 2\pi/N$ can be interpreted as a consequence of a finite diffusion length x_s. This simply means that steps separated by N steps or more cannot be coupled via adatom diffusion. Let us estimate this cutoff N. The adatom motion can be seen as the result of hopping between steps with the mean velocity $v_\perp$. This velocity is the result of diffusion and attachment kinetics. Thus we have $v_\perp^{-1} \simeq l/D + \nu_+^{-1} + \nu_-^{-1}$. After each hop the adatom ''choose'' arbitrarily to go to one of its two neighbors. Therefore, the resulting adatom motion is Brownian. A well-known result for Brownian motion is that the departure from the initial position of the particle is proportional to the square root of the number of hops. The number of hops needed to go from one position to another, N steps further, is therefore N^2. The distance covered by an adatom before desorption is $v_\perp \tau = N^2 l$ and the cutoff N is given by $N = x_s/\sqrt{l(l + d_+ + d_-)}$. We insert this relation into the expression of ΩF_{BZ} [Eq. 61)] as a function of the cutoff. We find

$$\Omega \tau F_{BZ} \simeq (2\pi)^2 \frac{2\Gamma(l + d_+ + d_-)}{(d_+ - d_-)l}. \quad (63)$$

This expression is in agreement with Eq. (52) in the large τ limit, which gives the same result, without the $(2\pi)^2$ prefactor. Many other phenomena can lead to this kind of cutoff, such as a vacancy or defect nucleation. This study is generic and shall be the framework of future developments that take into account phenomena leading to nonconserved dynamics at large scales.

VI. SUMMARY

A general conclusion together with an outlook is presented in the following paper. Here we simply sum up the main results. This paper has dealt with the general formulation of dynamics on a vicinal surface during MBE growth. The model uses that of Burton, Cabrera, and Frank[11] supplemented with elasticity, noninstantaneous and asymmetric (the Ehrlich-Schwœbel effect) adatoms kinetics at the steps, and an appropriate Langevin formalism. The noise sources that are involved are the shot noise, diffusion noise, and

noise associated with attachment/detachment at the steps. The full formalism has been tested at equilibrium. This was a necessary check for the self-coherence of the model. Several features at equilibrium were recovered and some other aspects discovered. A more extensive discussion in that regime is presented in Ref. 16. Out of equilibrium we have identified a diffusive repulsion that prevails in most realistic cases over the elastic repulsion. This has led to the derivation of a scaling law for step wandering. The diffusive repulsion partially orders the train fluctuation; terrace width fluctuations together with step wandering are significantly reduced by nonequilibrium effects. This discovery is not devoid of experimental testability. When the system is driven further away from equilibrium by increasing the incoming flux, the steps suffer a morphological instability. We have given a transparent picture of what fixes the critical flux. At the instability threshold, fluctuations diverge. We have shown how the divergence occurs as a function of the system size and the distance from the threshold. At the instability threshold, nonlinear effects can no longer be disregarded. This part is the subject of the following paper.

ACKNOWLEDGMENTS

We are grateful to T. Ihle, A. Karma, J. Krug, P. Nozières, J. Villain, and A. Pimpinelli for several enlightening discussions. We are grateful to the Center Grenoblois de Calcul Vectoriel for providing us with computing facilities. Part of the work of O.P.L. was supported by NSF-sponsored MRSEC, Grant No. DMR 96-32521.

APPENDIX A: AMPLITUDE OF THE LANGEVIN FORCES

At equilibrium the flux is $F_{eq}=c^0_{eq}/\tau$ and the concentration c fluctuates around the mean value c^0_{eq}. According to Eq. (5), these fluctuations obey

$$\frac{\partial}{\partial t}(c-c^0_{eq})=D\nabla^2(c-c^0_{eq})-\frac{c-c^0_{eq}}{\tau}+f-\boldsymbol{\nabla}\cdot\mathbf{q}. \quad \text{(A1)}$$

This leads to the static spectrum of the equilibrium fluctuations

$$\langle (c-c^0_{eq})_k (c-c^0_{eq})_{-k}\rangle=\frac{1}{2}\,\frac{k^2B_c+B_n}{Dk^2+1/\tau}, \quad \text{(A2)}$$

where the correlations of the Langevin forces are written as

$$\langle q_{mi}(\mathbf{r},t)q_{m'j}(\mathbf{r}',t')\rangle=B_c\delta\delta_{ij}, \quad \text{(A3)}$$

$$\langle f_m(\mathbf{r},t)f'_m(\mathbf{r}',t')\rangle=B_n\delta, \quad \text{(A4)}$$

where δ is an abbreviation for $\delta(\mathbf{r}-\mathbf{r}')\delta(t-t')\delta_{m,m'}$ and i,j stand for x or z. Moreover, we know[22] that

$$\langle (c-c^0_{eq})(\mathbf{r},t)(c-c^0_{eq})(\mathbf{r}',t')\rangle=c^0_{eq}\delta(\mathbf{r}-\mathbf{r}')\delta(t-t'). \quad \text{(A5)}$$

Confronting Eq. (A2) with Eq. (A5), we obtain

$$B_c=2Dc^0_{eq}, \quad \text{(A6)}$$

$$B_n=2\frac{c^0_{eq}}{\tau}. \quad \text{(A7)}$$

The correlation laws of the attachment/detachment noise η are calculated in a similar way. A linearization of Eq. (14) provides us with the evolution equation of the meander at equilibrium

$$\frac{\partial\zeta_m}{\partial t}=\frac{D}{d_+}\left[\Omega\eta_+-\Gamma\kappa-\frac{A}{l^4}(2\zeta_m-\zeta_{m+1}-\zeta_{m-1})\right]+\frac{D}{d_-}\left[\Omega\eta_--\Gamma\kappa-\frac{A}{l^4}(2\zeta_m-\zeta_{m+1}-\zeta_{m-1})\right]. \quad \text{(A8)}$$

We then calculate the static spectrum of the meander ζ in Fourier space

$$\langle\zeta_{k\Phi}\zeta_{-k-\Phi}\rangle=\frac{D}{d_+d_-}\,\frac{d_+^2B_{\eta_+}+d_-^2B_{\eta_-}}{2(d_++d_-)\left(\Gamma k^2+2\frac{A}{l^4}(1-\cos(\Phi))\right)}, \quad \text{(A9)}$$

where the amplitude B_{η_+} and B_{η_-} are defined by

$$\langle\eta_{m\pm}(\mathbf{r},t)\eta_{m'\pm}(\mathbf{r}',t')\rangle=B_{\eta_\pm}\delta. \quad \text{(A10)}$$

At equilibrium we must recover Eq. (33), where the phase ϕ designates the Fourier conjugate variable of the discrete label of the steps m. Comparing this static spectrum to the one obtained by Eq. (A8) fixes the amplitudes of the attachment noises

$$B_{\eta_\pm}=\frac{2c^0_{eq}}{\nu_\pm}. \quad \text{(A11)}$$

The amplitude of the Langevin forces have been calculated at equilibrium. We use a local thermodynamic equilibrium approximation, which allows one to extend the above noise forces to the out-of-equilibrium case.[23] The Langevin forces are thus obtained by substituting in the above relations c^0_{eq} by c:

$$\langle q_{mi}(\mathbf{r},t)q_{m'j}(\mathbf{r}',t')\rangle=2Dc(\mathbf{r},t)\delta\delta_{ij}, \quad \text{(A12)}$$

$$\langle f_m(\mathbf{r},t)f_{m'}(\mathbf{r}',t')\rangle=2\,\frac{c(\mathbf{r},t)}{\tau}\,\delta, \quad \text{(A13)}$$

$$\langle\eta_{m\pm}(x,t)\eta_{m'\pm}(x',t')\rangle=\frac{2c_\pm(x,t)}{\nu_\pm}\delta(x-x')\delta(t-t')\delta_{mm'}, \quad \text{(A14)}$$

where $c_\pm$ is the concentration on both sides of the step. This implies that we consider features on spatial and temporal scales that are large in comparison to the mean free paths and collision frequencies (the traditional hydrodynamical limit).

APPENDIX B: GREEN'S FUNCTION FORMALISM

1. Green's function

Equations (5), (6), and (14) completely describe the dynamics of the vicinal surface. It is possible to convert them into an integral form by means of Green's function techniques. For convenience we use the normalized concentration $u=\Omega(c-\tau F)$ instead of the concentration c. Equation (5) then becomes

$$\frac{\partial u}{\partial t}=V\frac{\partial u}{\partial z}+D\nabla^2 u-\frac{u}{\tau}+\Omega(f-\boldsymbol{\nabla}\cdot\mathbf{q}), \tag{B1}$$

where we have written it in a frame moving with the velocity V corresponding to the uniform train. The free propagator associated with Eq. (5) satisfies the equation

$$\left(\tau D\nabla^2-1+\tau\frac{\partial}{\partial t'}-\tau V\frac{\partial}{\partial z'}\right)G(\mathbf{r}-\mathbf{r}',t-t') =-\delta(\mathbf{r}-\mathbf{r}')\,\delta(t-t'). \tag{B2}$$

To determine G we take the Fourier transform of Eq. (B2), which is defined by

$$\hat{G}(\mathbf{k},\omega)=\int_{-\infty}^{\infty}dt'\int\int d^2\mathbf{r}'G(\mathbf{r}-\mathbf{r},t-t') \times e^{i\omega(t-t')+i\mathbf{k}\cdot(\mathbf{r}-\mathbf{r}')}. \tag{B3}$$

$\hat{G}$ obeys the equation

$$(-\tau D\mathbf{k}^2+i\tau Vk_z-i\omega\tau-1)\hat{G}(\mathbf{k},\omega)=-1. \tag{B4}$$

The Green's function then reads

$$G(\mathbf{r}-\mathbf{r}',t-t') =\int_{-\infty}^{+\infty}\frac{d\omega}{2\pi}\int\int\frac{d^2k}{(2\pi)^2}\frac{e^{-i\omega(t-t')-i\mathbf{k}\cdot(\mathbf{r}-\mathbf{r})}}{1+\tau D\mathbf{k}^2+i(\omega\tau-\tau Vk_z)}, \tag{B5}$$

which is easily integrated to yield Eq. (23). We multiply Eq. (B2) by u and Eq. (B1) by G and we take the difference. Then we integrate this expression in space over a terrace (Fig. 6) and in time from $-\infty$ to $t-\epsilon$. The resulting equation is written as

$$0=\int_{-\infty}^{t-\epsilon}dt'\int\int d^2\mathbf{r}'[\tau D(G\nabla^2u'-u'\nabla^2G)] +\int_{-\infty}^{t-\epsilon}dt'\int\int d^2\mathbf{r}'\left[\tau V\frac{\partial}{\partial z'}(Gu')-\tau\frac{\partial}{\partial t'}(Gu')\right] +\Omega\tau\int_{-\infty}^{t-\epsilon}dt'\int\int d^2\mathbf{r}'(f-\boldsymbol{\nabla}q)G. \tag{B6}$$

Since G depends on both the $\mathbf{r}-\mathbf{r}'$ and $t-t'$ we shall omit it to specify the arguments. For the other quantities a prime indicates that the arguments are t', x', and z'. Using simple manipulations together with use of properties of the Green's function G,

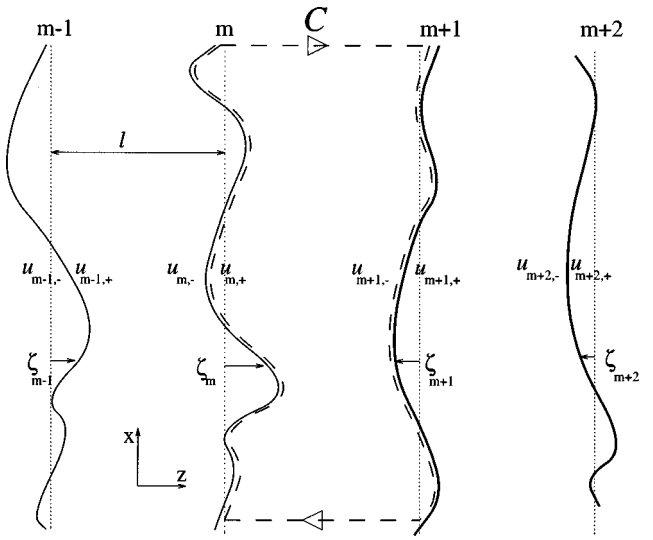

FIG. 6. The steps are labeled with the index m. The normalized concentrations on both sides of the steps are $u_{m,+}$ and $u_{m,-}$. In the Green's formalism expressions, the integration is made along the contour C (dashed line).

$$\lim_{\epsilon\to 0}G(\mathbf{r}-\mathbf{r}',\epsilon)=\frac{1}{\tau}\delta(\mathbf{r}-\mathbf{r}'), \tag{B7}$$

$$\lim_{t'\to\infty}G(\mathbf{r}-\mathbf{r}',t-t')=0, \tag{B8}$$

we obtain

$$u(\mathbf{r},t)=\int_{-\infty}^{t}dt'\Bigg[\tau\int_{-\infty}^{\infty}dx'(V+\dot{\zeta}')u'G +D\tau\int d\Gamma_s'\left(G\frac{\partial u'}{\partial n'}-u'\frac{\partial G}{\partial n'}\right)\Bigg]_{z'=ml+\zeta_m'}^{z'=(m+1)l+\zeta_{m+1}'} +\Omega\tau\int_{-\infty}^{t}dt'\int_{-\infty}^{\infty}dx' \times\int_{ml+\zeta_m}^{(m+1)l+\zeta_{m+1}}dz'(f'-\boldsymbol{\nabla}'\cdot\mathbf{q}')G. \tag{B9}$$

$d\Gamma_s'$ is the step arclength element. In the above equation, the concentration on a terrace is calculated as a function of the concentration at the adjacent steps and their normal derivatives. The quantity $\mathbf{r}$ can be any point on a terrace. When taking the limit $\mathbf{r}=\mathbf{r}_{step}$ care should be taken since due to the discontinuity of $\partial G/\partial n'$, which gives an extra contribution, $\int\partial G/\partial n'\,h'\,d\Gamma_s'|_{terrace}=1/2h|_{step}+\int\partial G/\partial n'\,h'\,d\Gamma_s'|_{step}$. Indeed, an analysis of this integral close to the step shows a δ-function contribution on one side of the step, which produces the term $1/2h|_{step}$. This is usually known as the double layer theorem.[24] Evaluating the integral equation at the step, we obtain two equations for $z=\zeta_m+ml$ and $z=\zeta_{m+1}+(m+1)l$. They take the form of Eq. (22).

2. Linear analysis

The zeroth-order field u on both sides of the steps and the mean velocity of the train are obtained to leading order. They are given by

$$u_{0+} = -\sigma\Omega c_{eq}^0 \frac{d_+ + d_- \cosh(l/x_s) + x_s \sinh(l/x_s)}{(d_+ + d_-)\cosh(l/x_s) + (x_s + d_+ d_-/x_s)\sinh(l/x_s)},$$

$$u_{0-} = -\sigma\Omega c_{eq}^0 \frac{d_- + d_+ \cosh(l/x_s) + x_s \sinh(l/x_s)}{(d_+ + d_-)\cosh(l/x_s) + (x_s + d_+ d_-/x_s)\sinh(l/x_s)}, \tag{B10}$$

$$V = \sigma\Omega c_{eq}^0 \left(\frac{D}{\tau}\right)^{1/2} \frac{2x_s[\cosh(l/x_s)-1] + (d_+ + d_-)\sinh(l/x_s)}{(d_+ + d_-)\cosh(l/x_s) + (x_s + d_+ d_-/x_s)\sinh(l/x_s)}.$$

The expression of the susceptibility and of the resulting noise involved in Eq. (27) are provided. In Fourier space, the inverse of the susceptibility is

$$\begin{aligned}\chi_{\omega k\Phi}^{-1} = {} & i\omega + \frac{D\Lambda_{\omega k}}{\mathcal{D}}\left(\Gamma k^2 + 2\frac{A}{l^4}[1-\cos(\Phi)]\right)\{2[\cosh(\Lambda_{\omega k} l)-1] + \Lambda_{\omega k}(d_+ + d_-)\sinh(\Lambda_{\omega k} l) + 2[1-\cos(\Phi)]\} \\ & + \frac{\Omega c_{eq}^0 \sigma}{\tau \mathcal{D}\mathcal{D}_0}\left(\frac{d_+ - d_-}{x_s}\left\{\Lambda_{\omega k}(d_+ + d_-)\left[x_s \Lambda_{\omega k}\sinh\left(\frac{l}{x_s}\right)\sinh(\Lambda_{\omega k} l) - \cosh\left(\frac{l}{x_s}\right)\cosh(\Lambda_{\omega k} l) + \cos(\Phi)\right] + \left[\cosh\left(\frac{l}{x_s}\right) - 1\right]\right.\right. \\ & \left.\left. \times [(x_s \Lambda_{\omega k})^2 - 1]\sinh(\Lambda_{\omega k} l)\right\} - i\,\sin(\Phi)\frac{\Lambda_{\omega k}}{x_s}\left[d_+^2 + d_-^2 - 2x_s^2 + 2(d_+ d_- + x_s^2)\cosh\left(\frac{l}{x_s}\right) + 2x_s(d_+ + d_-)\sinh\left(\frac{l}{x_s}\right)\right]\right),\end{aligned} \tag{B11}$$

where we have used the notations

$$\sigma = \tau F/c_{eq}^0 - 1,$$

$$\Lambda_{\omega k} = \sqrt{i\omega/D + k^2 + 1/x_s^2},$$

$$\mathcal{D}_0 = \frac{d_+ + d_-}{x_s}\cosh\left(\frac{l}{x_s}\right) + \left(\frac{d_+ d_-}{x_s^2} + 1\right)\sinh\left(\frac{l}{x_s}\right), \tag{B12}$$

$$\mathcal{D} = (d_+ + d_-)\Lambda_{\omega k}\cosh(\Lambda_{\omega k} l) + (d_+ d_- \Lambda_{\omega k}^2 + 1)\sinh(\Lambda_{\omega k} l).$$

The resulting noise that enters Eq. (27) is written in Fourier space as a function of the Langevin forces introduced before:

$$\begin{aligned}\beta_{\omega k\Phi} = {} & \frac{\Omega D\Lambda_{\omega k}}{\mathcal{D}}\{[\cosh(\Lambda_{\omega k} l) + \Lambda_{\omega k} d_- \sinh(\Lambda_{\omega k} l) - e^{-i\Phi}]\eta_{+,\omega k\Phi} + [\cosh(\Lambda_{\omega k} l) + \Lambda_{\omega k} d_+ \sinh(\Lambda_{\omega k} l) - e^{i\Phi}]\eta_{-,\omega k\Phi}\} \\ & + \frac{\Omega}{\mathcal{D}}\int_0^l dz'\,(\sinh[\Lambda_{\omega k}(l-z')] + \Lambda_{\omega k} d_- \cosh[\Lambda_{\omega k}(l-z')] + e^{-i\Phi}[\sinh(\Lambda_{\omega k} z') + \Lambda_{\omega k} d_+ \cosh(\Lambda_{\omega k} z')][f_{\omega k\Phi}(z') \\ & - ikq_{x,\omega k\Phi}(z')] - \{\cosh[\Lambda_{\omega k}(l-z')] + \Lambda_{\omega k} d_- \sinh[\Lambda_{\omega k}(l-z')] - e^{-i\Phi}[\cosh(\Lambda_{\omega k} z') \\ & + \Lambda_{\omega k} d_+ \sinh(\Lambda_{\omega k} z')]\}\Lambda_{\omega k} q_{z,\omega k\Phi}(z')).\end{aligned} \tag{B13}$$

APPENDIX C: OUT-OF-EQUILIBRIUM STEP ROUGHNESS AND INTERSTEP CORRELATIONS

We have calculated the step roughness and the interstep correlations in the quasistatic approximation. The step roughness is given by Eq. (28), where use is made of Eqs. (B11) and (B13) in a long-wavelength limit. For small enough fluxes, the equilibrium part of the noise amplitude dominates. When the diffusive repulsion is stronger than the elastic one and if the step stiffness overcomes the diffusive instability,

$$\frac{w^2}{\Omega^2 c_{eq}^0}=\int_{-\infty}^{+\infty}\frac{dk}{2\pi}\int_0^{2\pi}\frac{d\Phi}{2\pi}\frac{f_0+2[1-\cos(\Phi)]}{\Gamma(1-\sigma/\sigma_{BZ})k^2 f_0+[1-\cos(\Phi)]\left[2\Gamma\left(1+\frac{\sigma}{\sigma_0}\right)k^2+\frac{\Omega c_{eq}^0\sigma d^2}{\mathcal{D}_0 x_s^3}\right]}, \tag{C1}$$

where we have defined

$$d=\sqrt{d_-^2-d_+^2},$$

$$\sigma_0=\frac{4\Gamma}{\Omega c_{eq}^0}\frac{\mathcal{D}_0}{d^2}x_s, \tag{C2}$$

$$f_0=\frac{d_++d_-}{x_s}\sinh(l/x_s)+2[\cosh(l/x_s)-1].$$

The roughness is

$$\frac{w^2}{\Omega}=\frac{x_s^{3/2}\mathcal{D}_0^{1/2}}{d\sqrt{2\sigma(\Gamma/\Omega c_{eq}^0)}}\left\{\frac{1}{\left(1+\frac{\sigma}{\sigma_0}\right)^{1/2}}\frac{2}{\pi}\arcsin\left[\left(1+\frac{1-\frac{\sigma}{\sigma_{BZ}}}{1+\frac{\sigma}{\sigma_0}}\frac{f_0}{4}\right)^{-1/2}\right]+\frac{1}{\left(1-\frac{\sigma}{\sigma_{BZ}}\right)^{1/2}}\left(\frac{f_0}{4}\right)^{1/2}\frac{2}{\pi}\right.$$

$$\left.\times\operatorname{arcsinh}\left[\frac{L}{2\pi}\frac{d}{x_s^{3/2}\mathcal{D}_0^{1/2}}\frac{[2\sigma/(\Gamma/\Omega c_{eq}^0)]^{1/2}}{\sqrt{\left(1-\frac{\sigma}{\sigma_{BZ}}\right)\frac{f_0}{4}+\left(1+\frac{\sigma}{\sigma_0}\right)}}\right]\right\}. \tag{C3}$$

The dependence on $\epsilon=1-\sigma/\sigma_{BZ}$ implies that close to the instability threshold (small ϵ) the squared roughness behaves like $w^2\sim\epsilon^{-1/2}$ and thus

$$w\sim\epsilon^{-1/4}. \tag{C4}$$

In the limit where desorption is small, expression (C3) reduces to

$$\frac{w^2}{\Omega}=\left(\frac{\Omega c_{eq}^0 x_s^2(l+d_++d_-)}{2\Gamma\sigma d^2}\right)^{1/2}\left\{\left(1+\frac{\sigma}{\sigma_0}\right)^{-1/2}+\epsilon^{-1/2}\frac{[l(l+d_++d_-)]^{1/2}}{2x_s}\frac{2}{\pi}\right.$$

$$\left.\times\operatorname{arcsinh}\left[\frac{L}{2\pi}\left(\frac{2d^2\sigma}{\Gamma x_s^2(l+d_++d_-)\left(1+\frac{\sigma}{\sigma_0}\right)}\right)^{1/2}\right]\right\}, \tag{C5}$$

with $\sigma_0=4\Gamma(l+d_++d_-)/\Omega c_{eq}^0 d^2$ in this limit.

In a similar manner, the interstep correlations defined by Eq. (41) are calculated under the same conditions as those that have led to Eq. (C1),

$$\frac{G(p)}{\Omega}=\left(\frac{\Omega c_{eq}^0 x_s^3\mathcal{D}_0}{d^2\sigma\Gamma\left(1+\frac{\sigma}{\sigma_0}\right)^{1/2}}\right)I(p). \tag{C6}$$

We have defined

$$I(p)=\int_0^{2\pi}\frac{d\Phi}{2\pi}\frac{\{f_0+2[1-\cos(\Phi)]\}[1-\cos(p\Phi)]}{\{g_0+2[1-\cos(\Phi)]\}^{1/2}[1-\cos(\Phi)]^{1/2}}, \tag{C7}$$

where

$$g_0 = f_0 \frac{1-\frac{\sigma}{\sigma_{BZ}}}{1+\frac{\sigma}{\sigma_0}}. \tag{C8}$$

Note that unlike the roughness, the correlations do not diverge with the length of the steps, but there is still a divergence for large p, where $G(p) \sim \ln[p]$. To show the logarithmic divergence of $I(p)$, we shall first note that

$$\begin{aligned} &I(p+1)-I(p) \\ &= \sqrt{2g_o}\int_0^\pi \frac{d\Phi}{\pi}\left(1+\frac{4}{g_0}\sin^2(\Phi)\right)^{1/2}\sin[(2p+1)\Phi] \\ &\quad + \sqrt{\frac{2}{g_0}}(f_0-g_0)\int_0^\pi \frac{d\Phi}{\pi}\frac{\sin[(2p+1)\Phi]}{\left(1+\frac{4}{g_0}\sin^2(\Phi)\right)^{1/2}} \end{aligned} \tag{C9}$$

and $I(0)=0$, so that we have integrals of the form

$$J(p) = \int_0^\pi d\Phi h[q^2\sin^2(\Phi)]\sin[(2p+1)\Phi], \tag{C10}$$

where h is a regular function of $q^2\sin^2(\Phi)$ and $q^2=4/g_0$. Using a Taylor expansion of h,

$$\begin{aligned} J(p) &= \int_0^\pi d\Phi \sum_{n=0}^{\infty} [q^2\sin^2(\Phi)]^n h_n \sin[(2p+1)\Phi] \\ &= \sum_{n=0}^{\infty} h_n q^{2n} U_{np} \\ &= \frac{1}{2p+1}\sum_{n=0}^{\infty}\left(\frac{q}{2p+1}\right)^{2n} h_n' \\ &\underset{p\to\infty}{\sim} \frac{1}{2p+1}h_0', \end{aligned} \tag{C11}$$

where we have defined $U_{np}=\int_0^\pi (d\Phi/\pi)\sin^{2n}(\Phi)\sin[(2p+1)\Phi]$, which is easily integrated $U_{np}=(2/\pi)(2n)!/(2p+1)^{2n+1}$. h_n and h_n' are functions of n. Thus $I(p+1)-I(p)\sim 1/(2p+1)$ for large p and then $I(p)\sim\ln(p)$.

Since $I(0)=0$, we can calculate the terrace width fluctuations $G_D(1)$ with the help of Eq. (C9) for $p=1$:

$$\begin{aligned} \frac{G_D(1)}{\Omega} &= \frac{x_s^{3/2}\mathcal{D}_0^{1/2}}{d\sqrt{2\sigma(\Gamma/\Omega c_{eq}^0)}}\frac{1}{\left(1+\frac{\sigma}{\sigma_0}\right)^{1/2}}\frac{2}{\pi} \\ &\quad\times\{\sqrt{g_0}+(2+f_0-g_0/2)\arcsin[(1+g_0/4)^{-1/2}]\}. \end{aligned}$$

In the case of small desorption

$$\frac{G_D(1)}{\Omega} = 2\left(\frac{(d_+ + d_- + l)x_s^2}{2\sigma(d_-^2-d_+^2)(\Gamma/\Omega c_{eq}^0)\left(1+\frac{\sigma}{\sigma_0}\right)}\right)^{1/2} \tag{C12}$$

so that, since $\langle \zeta_m(\mathbf{r},t)\zeta_{m+1}(\mathbf{r},t)\rangle = w^2 - G(1)/2$,

$$\begin{aligned} &\langle \zeta_m(\mathbf{r},t)\zeta_{m+1}(\mathbf{r},t)\rangle \\ &\quad = \frac{l}{\pi x_s}\left(\frac{1}{1-\frac{\sigma}{\sigma_{BZ}}}\right)^{1/2} \\ &\qquad \times \operatorname{arcsinh}\left[\frac{L}{2\pi}\left(\frac{2d^2\sigma}{\Gamma x_s^2(l+d_++d_-)\left(1+\frac{\sigma}{\sigma_0}\right)}\right)^{1/2}\right]. \end{aligned}$$

Far from the morphological instability ($\sigma \ll \sigma_{BZ}$), $2w^2 \simeq G_D(1)$ (because $l \ll x_s$), the terrace width fluctuation is equal to the sum of the fluctuations of its neighboring steps. The steps seem to be uncorrelated. When the supersaturation increases and reaches the instability threshold, w^2 diverges but $G_D(1)$ does not. This means that the terraces are still well defined when the morphological instability occurs. This is not contradictory since the first unstable mode is the in-phase mode.

*Present address: Physics Department, University of Maryland, College Park, MD 20742-4111.

[1] B. S. Swartzentruber, Y. W. Mo, R. Kariotis, M. G. Lagally, and M. B. Webb, Phys. Rev. Lett. **65**, 1913 (1990).
[2] See, for example, P. Nozières, in *Solids Far From Equilibrium* (Cambridge University Press, Cambridge, 1991).
[3] E. E. Gruber and W. W. Mullins, J. Phys. Chem. Solids **28**, 875 (1967); B. S. Swartzentruber, Y. W. Mo, R. Kariotis, M. G. Lagally, and M. B. Webb, Phys. Rev. Lett. **65**, 1913 (1990).
[4] V. I. Marchenko and A. Ya. Parshin, Sov. Phys. JETP **52**, 129 (1980).
[5] N. C. Bartelt, J. L. Goldberg, T. L. Einstein, and E. D. Williams, Surf. Sci. Lett. **240**, L591 (1990); N. C. Bartelt, J. L. Goldberg, T. L. Einstein, and E. D. Williams, Surf. Sci. **273**, 252 (1992).
[6] O. Pierre-Louis and C. Misbah, Phys. Rev. Lett. **76**, 4761 (1996).
[7] R. L. Schwœbel, J. Appl. Phys. **40**, 614 (1969).
[8] G. S. Bales and A. Zangwill, Phys. Rev. B **41**, 5500 (1990).
[9] W. W. Mullins and R. F. Sekerka, J. Appl. Phys. **35**, 444 (1964).
[10] M. Uwaha and Y. Saito, Phys. Rev. Lett. **68**, 224 (1992).
[11] W. K. Burton, N. Cabrera, and F. C. Frank, Philos. Trans. R. Soc. London, Ser. A **243**, 299 (1951).
[12] T. Salditt and H. Spohn, Phys. Rev. E **47**, 3524 (1993).
[13] C. Misbah and W. J. Rappel, Phys. Rev. B **48**, 12 193 (1993).
[14] Fong Liu and H. Metiu, Phys. Rev. E **49**, 2601 (1994).
[15] I. Bena, C. Misbah, and A. Valance, Phys. Rev. B **47**, 7408 (1993).
[16] T. Ihle, C. Misbah, and O. Pierre-Louis, this issue, Phys. Rev. B **58**, 2289 (1998).
[17] J. Villain, D. R. Grempel, and J. Lapujoulade, J. Phys. F **15**, 809 (1985).
[18] J. C. Heyraud, J. M. Bermond, C. Alfonso, and J. J. Métois, J. Phys. I **5**, 443 (1995).

[19] C. Alfonso, J. M. Bermond, J. C. Heyraud, and J. J. Métois, Surf. Sci. **262**, 371 (1992).
[20] J. Krug and M. Schimschak, J. Phys. I **5**, 1065 (1995).
[21] A. Karma and C. Misbah, Phys. Rev. Lett. **71**, 3810 (1993).
[22] L. D. Landau and E. M. Lifshitz, *Theoretical Physics V, Statistical Physics* (Pergamon, Oxford, 1967), Pt. 1, Sec. 113.
[23] P. C. Hohenberg and J. B. Swift, Phys. Rev. A **46**, 4773 (1992). In the context of solidification from a melt, the problem was treated recently by A. Karma, Phys. Rev. E **48**, 3441 (1993).
[24] See, for example, G. Dee and R. Mathur, Phys. Rev. B **27**, 7073 (1983).